

# Theoretical and Experimental Investigation of Novel Varactor-Tuned Switchable Microstrip Ring Resonator Circuits

T. SCOTT MARTIN, FUCHEN WANG, AND KAI CHANG, SENIOR MEMBER, IEEE

**Abstract**—A novel microstrip ring resonator circuit loaded with two p-i-n diodes has been developed as a switchable filter. By replacing one p-i-n diode with a varactor diode, the switchable filter can be made electronically tunable. Isolation exceeding 20 dB with 9 percent tuning bandwidth was demonstrated. An analysis based on transmission line theory was used to model both circuits. The analysis includes the effects of diode parasitics, coupling gaps, dispersion, and mounting gap capacitance. The experimental results agree very well with the theoretical calculation.

## I. INTRODUCTION

**M**ICROSTRIP ring resonators have been widely used for the measurements of dispersion, phase velocity, and dielectric constant [1]–[4]. The ring resonator alone naturally acts as a bandpass filter. The frequencies that pass through the circuit are only those whose guided wavelength is an integral multiple of the mean circumference. If gaps are cut at 90° radially from the feed point, as shown in Fig. 1, the odd-numbered modes disappear and only the even-numbered modes appear in order to satisfy the boundary conditions. Varactor-tuned ring resonators were recently demonstrated with up to 15 percent tuning range by mounting varactor diodes in the gaps [5], [6].

This paper reports two novel ring circuits: an electronically switchable filter and a tunable switchable filter using p-i-n diodes. The p-i-n diode acts as an open circuit when reverse biased and a short circuit when forward biased. If the diodes are mounted across the gaps in the ring resonator shown in Fig. 1, the odd modes can be switched on and off by varying the bias on the diode. When the diodes are forward biased, it is as if there were no gaps in the ring and all integer numbered modes were passed. When the diodes are reverse biased, the boundary conditions will not allow the odd-numbered modes to propagate and they will have a high attenuation. High isolation is thus achieved

Manuscript received March 11, 1988; revised July 12, 1988. This work was supported by the Office of Naval Research under Contract N00014-86-K-0348.

T. S. Martin was with the Department of Electrical Engineering, Texas A&M University, College Station, TX. He is now with the Microwave Laboratory, Texas Instruments, Dallas, TX.

F. Wang and K. Chang are with the Department of Electrical Engineering, Texas A&M University, College Station, TX 77843-3128.

IEEE Log Number 8823774.

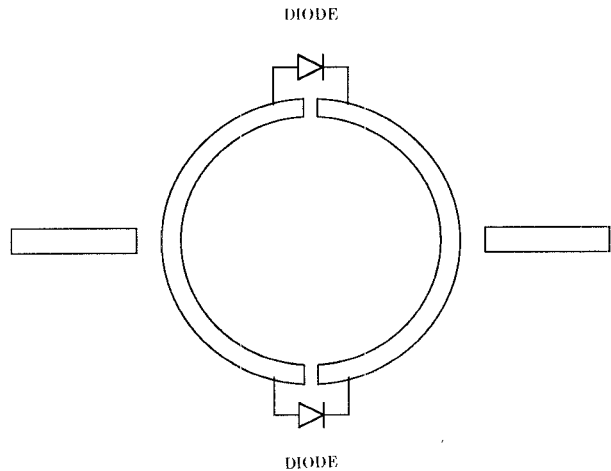


Fig. 1. Circuit configuration of a resonant ring mounted with two diodes.

due to built-in mode rejection. A switchable ring resonator was built with less than 2 dB insertion loss and over 20 dB isolation.

If a varactor diode is used to replace one of the two p-i-n diodes, the switchable filter can be made tunable. This circuit would have not only an electronically tunable resonant frequency but also a resonant frequency that can be switched on and off. A tuning bandwidth of over 9 percent with over 20 dB isolation was demonstrated.

Although the microstrip ring resonators have been studied extensively in the open literature [7]–[10], most studies used a field theory approach to investigate the effects of line width, curvature, and dispersion on the resonant frequency. An open-ring resonator with a gap inside the ring was also investigated using a magnetic wall model and perturbation analysis [11], [12]. However, it is difficult to incorporate the varactor and p-i-n diodes into the analysis. To overcome these problems, a circuit analysis based on transmission line theory was used [6]. The analysis requires that each component, as well as the microstrip line, coupling gap, and any additional devices, be represented by its equivalent circuit model. The analysis includes the effects of coupling gaps, diode parasitics, dispersion, and mounting gap capacitance. The experimental results agree very

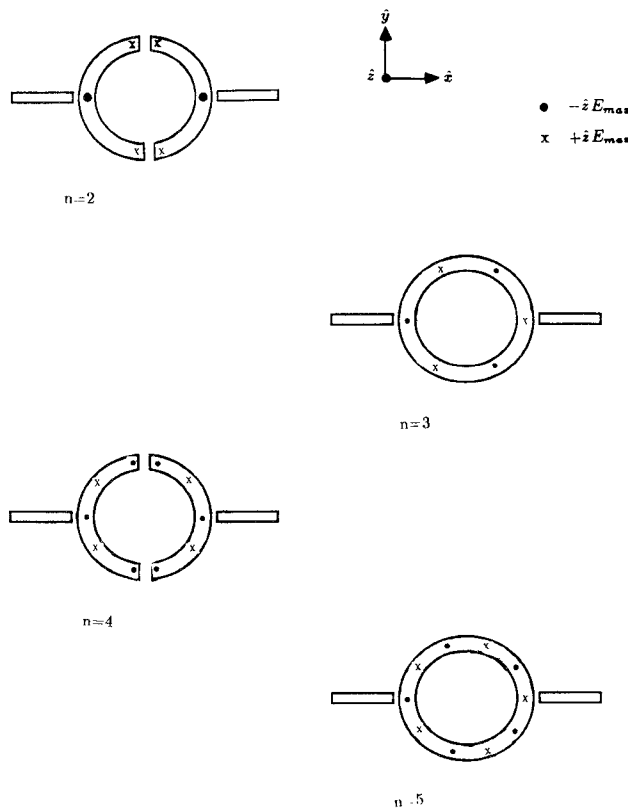


Fig. 2. Mode chart for a resonant ring with two cuts inside the ring.

well with the theoretical calculation. The errors in resonant frequency and tuning bandwidth predictions are within 3 percent.

Circuit modeling was used to study the effect of the package parasitics on the tuning range. For a maximum tuning range, it was found that the package capacitance should be as small as possible and the package inductance as large as possible. The bulk resistance has little effect on tuning range but should be small for low insertion loss.

Although the analysis does not include the conductor losses and radiation losses, it provides the input and output impedance information which can be used to design a broadband matching network. This matching circuit is necessary to reduce the *VSWR* and mismatch loss at resonance.

The ring circuit described here combines three functions in one device: filtering, tunability, and switchability. Since the device is monolithically compatible, the results should have many applications in hybrid and monolithic integrated circuits.

## II. ELECTRONICALLY SWITCHABLE RING RESONATORS

It is well known that the ring resonator exhibits a bandpass/band-reject frequency response. The modes (or frequencies) that pass through the circuit are only those whose guided wavelength is an integral multiple of the mean circumference. The number of wavelengths present on the ring at resonance defines the mode numbers. There are infinitely many resonant frequencies and therefore

infinitely many mode numbers. These modes are not all equally affected when the ring circuit is changed. An example of this is to have a cut in the ring at 90° radially from the feed point. To satisfy the new boundary conditions the odd-numbered modes disappear and the new half-modes appear, as shown in [6, figure 10]. If it is possible to repair the cut so that the ring is complete again, the half-modes will disappear and the odd modes will reappear again. This idea can be used to develop a switchable resonator/filter. When a p-i-n diode is mounted across the gap, only the integer numbered modes are present (no half-modes) when the diode is forward biased. When the diode is reverse biased, the half-modes appear due to the boundary conditions (and the odd-numbered modes disappear).

For a circuit with two gaps as shown in Fig. 1, the odd-numbered modes disappear and only the even-numbered modes exist in order to satisfy the boundary conditions. The mode chart is shown in Fig. 2. If two p-i-n diodes are used for the circuit shown in Fig. 1, the resonant frequencies of the odd-numbered modes can be switched on and off electronically. The odd modes exist when the diodes are forward biased and disappear when the diodes are reverse biased.

The equivalent circuit of the diode loaded ring can be represented by Fig. 3. The transmission line is represented by a T network and the coupling gaps are modeled by a gap series capacitance ( $C_2$ ) together with two fringe capacitances ( $C_1$ ). The impedances  $Z_{top}$  and  $Z_{bot}$  represent the impedances of the p-i-n diodes. The equivalent circuit used to calculate  $Z_{top}$  and  $Z_{bot}$  is given in Fig. 4.  $R_f$  is the series resistance of the forward-biased diode. When reverse biased,  $C_j$  represents the junction capacitance and  $R_r$  is the series resistance.  $L_p$  is the lead inductance and  $C_p$  the packaged capacitance.  $L_s$  accounts for the inductance introduced by the bonding wire and  $C_2$  is the capacitance of the mounting gap.

The input impedance looking into the ring at the coupling gap can be calculated by solving the six loop equations as follows:

$$[V] = [Z][I]$$

where

$$[V] = \begin{pmatrix} V_{unit} \\ 0 \\ 0 \\ 0 \\ 0 \\ V_{unit} \end{pmatrix}$$

$$[I] = \begin{pmatrix} i_1 \\ i_2 \\ i_3 \\ i_4 \\ i_5 \\ i_6 \end{pmatrix}$$

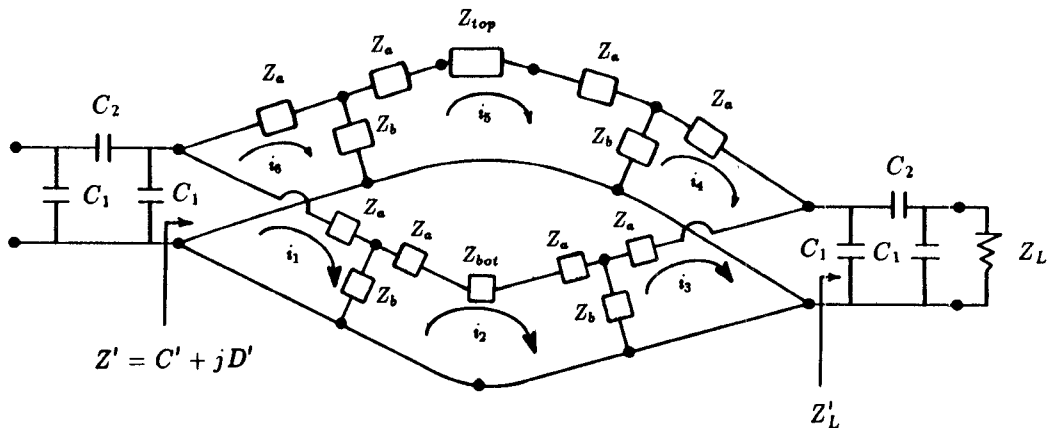


Fig. 3. Equivalent circuit of a resonant ring mounted with two diodes.

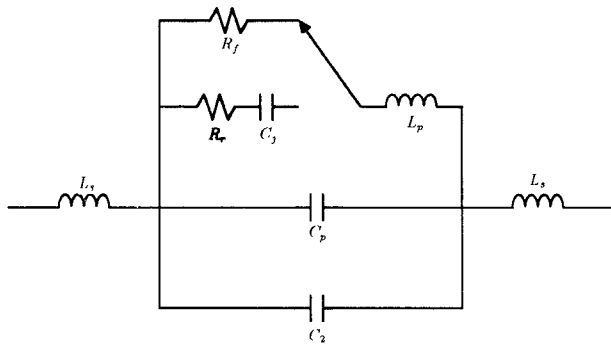


Fig. 4. Equivalent circuit of a p-i-n diode.

and

$$[Z] = \begin{pmatrix} Z_a + Z_b & -Z_b & 0 & 0 & 0 & 0 \\ -Z_b & 2Z_a + 2Z_b + Z_{bot} & -Z_b & 0 & 0 & 0 \\ 0 & -Z_b & Z_a + Z_b + Z'_L & Z'_L & 0 & 0 \\ 0 & 0 & Z'_L & Z_a + Z_b + Z'_L & -Z_b & 0 \\ 0 & 0 & 0 & -Z_b & 2Z_a + 2Z_b + Z_{top} & -Z_b \\ 0 & 0 & 0 & 0 & -Z_b & Z_a + Z_b \end{pmatrix}$$

Once the currents are known then

$$Z' = C' + jD' = \frac{V_{unit}}{i_1 + i_6}.$$

The input impedance of the circuit,  $Z_{in}$ , can be found from  $Z'$ . The input impedance can be used to design the matching networks for the tunable ring or tunable switchable ring circuits.

The resonant frequency can be determined in two ways. The first method is to use the bisection algorithm to determine the frequency at which  $X_{in} = 0$  ( $X_{in}$  is the imaginary part of  $Z_{in}$ ). The second method uses the  $S$  parameters of the circuit. The ratio of the reflected power over the incident power can be determined from

$$S_{11} = \frac{Z_{in} - Z_0}{Z_{in} + Z_0}$$

where  $Z_{in}$  is the input impedance of the circuit and  $Z_0$  is the characteristic impedance. From  $S_{11}$ , the ratio of transmitted power to incident power for a lossless circuit can be

determined from

$$S_{21} = \sqrt{1 - S_{11}^2} = S_{12}.$$

The resonant frequency is the point at which  $S_{12}$  reaches a maximum, resulting in maximum power transfer. For a lossless or low-loss case, the condition  $S_{12} = \max$  and  $X_{in} = 0$  occurs at nearly the same frequency and it is equally correct to apply either condition. The  $S$  parameter method is more useful if the attenuation at some frequency is desired. For a lossy case, solving  $X_{in} = 0$  will give better accuracy.

If the forward bias condition is considered and an odd-numbered mode is observed,  $S_{12}$  will reach a maximum at the resonant frequency. If the reverse bias condi-

tion is considered then the odd-numbered modes will have a much higher attenuation and there will be no resonance. The isolation is given by the difference in  $S_{12}$  at the resonant frequency for the forward bias condition and  $S_{12}$  at the same frequency for the reverse-biased condition.

A circuit was designed and fabricated based upon the analysis. It was built on a RT/Duroid 5880 substrate with the following dimensions:

substrate thickness:	0.762 mm
line width:	2.310 mm
coupling gap:	0.250 mm
device mounting gap:	0.250 mm
ring radius:	3.484 cm

The p-i-n diodes used were from MA/COM (model 47047) with  $L_p = 2.0 \text{ nH}$ ,  $C_p = 0.1 \text{ pF}$ ,  $C_j = 0.3 \text{ pF}$  at  $-50 \text{ V}$ , and  $R_f = 1.3 \Omega$  at  $100 \text{ mA}$ .  $L_s$  is estimated to be  $0.2 \text{ nH}$ . A value for  $R_r$  is not quoted, but similar diodes have a resistance of  $2 \Omega$ .

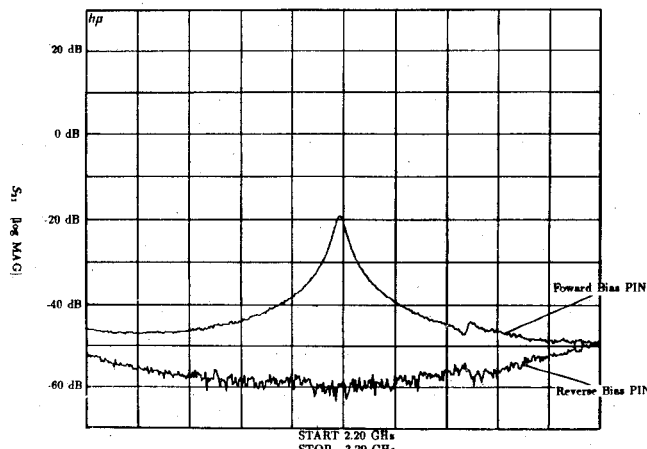


Fig. 5. Measured response of a switchable ring resonator.

Using the above parameters, the analysis predicts the resonant frequency for the third resonant mode to be 2.74 GHz when the diode is forward biased. The measured results shown in Fig. 5 indicate a resonant frequency of 2.69 GHz. The resonant frequency was accurately predicted to within a respectable 2 percent. Using simply the approximation  $2\pi r = n\lambda_g$ , the resonant frequency is calculated to be 3 GHz, which is off by 10 percent. Because the forward-biased p-i-n diode can be represented primarily by its package parasitics, it becomes very obvious that the parasitics and coupling gaps significantly affect the resonant frequency.

The results shown in Fig. 5 also indicate an excellent isolation. When the diodes are forward biased with a total current of 400 mA, the circuit has a resonance at 2.69 GHz. When the diodes are reverse biased to  $-50$  V, the mode is turned off and there is no resonance. The signal isolation at 2.69 GHz when the circuit is reverse biased is better than 40 dB. The high insertion loss is mainly due to the large coupling gap. To reduce the insertion loss, a much smaller coupling gap is required. The small gap will significantly improve the impedance matching and reduce the loss. Since fabrication tolerance limits the gap size to a minimum of about  $25 \mu\text{m}$ , an insulated copper tape was used to bridge the gap. The coupling capacitance is formed by the insulation material between the tape and the microstrip line. This capacitance is equivalent to a coupling gap size of less than  $3 \mu\text{m}$ . The circuit with insulated copper tape across the gap was tested and the results are shown in Fig. 6. The loss has been reduced to less than 2 dB in the "on" state with over 20 dB isolation in the "off" state. The resonant frequency was shifted from 2.69 GHz to 2.6 GHz as a result of the increased coupling capacitance.

### III. ELECTRONICALLY TUNABLE AND SWITCHABLE RING RESONATORS

A varactor mounted in a ring resonator circuit can be used to tune the resonant frequency of what has come to be known as the half-modes [6]. These half-modes arise because the varactor, which represents a high impedance

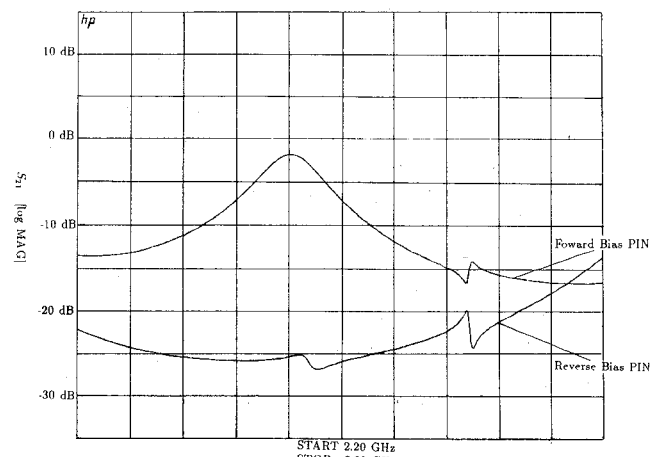


Fig. 6. Measured response of a switchable ring resonator with lower insertion loss.

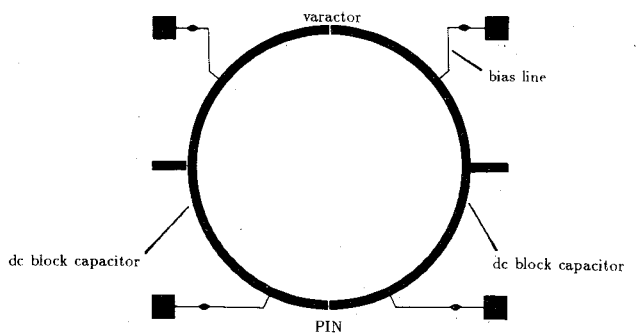


Fig. 7. Mask used for the tunable switch filter.

when reverse biased, is almost equivalent to an open circuit at the mounting position. This open circuit forces boundary conditions on the ring which allow the half-modes to appear and odd-numbered modes to disappear.

The half-modes could be turned off and on by correctly mounting a p-i-n diode in the circuit. The two states of the p-i-n diode, forward and reverse biased, present different boundary conditions on the ring to be satisfied. A forward-biased p-i-n diode represents a short circuit and the circuit behaves as a normal ring resonator with all integer numbered modes being present. When the p-i-n diode is reverse biased it represents an open circuit and the frequency response of the circuit is similar to the varactor mounted ring; the odd modes disappear and the half-modes appear.

A novel circuit is conceived when the properties of the varactor-tuned ring and the p-i-n diode switchable filter are combined in one circuit. This circuit has not only an electronically tunable resonant frequency but also a resonant frequency that can be switched on and off. The circuit used for the switchable filter has been modified to achieve tunability. The actual mask is shown in Fig. 7. The varactor and p-i-n diodes are to be mounted across the gaps cut at  $90^\circ$  radially from the feed lines. Across the remaining two cuts, large dc block capacitors are mounted. The dc block capacitors are necessary because the biases on the p-i-n and varactor diodes are different.

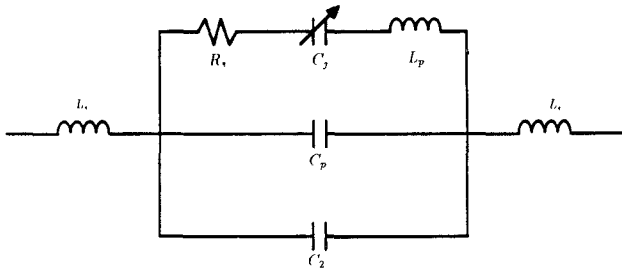


Fig. 8. Equivalent circuit of a packaged varactor.

A theoretical analysis was developed based on the same methods and equivalent circuits as in Section II. The  $Z_{top}$  in Fig. 3 is replaced by a varactor diode with equivalent circuit shown in Fig. 8. The particular mode of interest is the mode  $n = 3.5$ . When the p-i-n diode is forward biased, the half-mode is present. The voltage across the varactor can then be varied to adjust the resonant frequency. As the capacitance of the varactor is decreased the resonant frequency increases. When the p-i-n diode is reverse biased, the half-mode is turned off. The predicted isolation for the circuit is 20 dB.

The theoretical and experimental results for the tuning range are given in Fig. 9 for comparison. The error is approximately 3 percent. The varactor (MA/COM model 46600) used has  $C_p = 0.05$  pF,  $L_s = 1$  nH, and  $R_s = 1$   $\Omega$ , and  $C_j(V)$  varied from 0.5 to 3.0 pF. When the p-i-n diode is forward biased, the varactor presents a tuning range from 2.90 to 3.16 GHz. This is approximately a 9 percent tuning bandwidth. When the p-i-n diode is reverse biased, the mode is turned off, giving an isolation of approximately 20 dB.

The tuning range of the resonant ring can be significantly increased if the p-i-n diode is replaced by a varactor. In this case, the resonant frequency is tunable but no longer switchable. The results are shown in Fig. 10. The tuning range is increased to 15 percent. Again, the agreement between experimental results and theoretical predictions is quite good.

#### IV. EFFECTS OF THE VARACTOR PACKAGE PARASITICS ON TUNING RANGE

The package parasitics could affect the tuning range of a varactor-tuned ring. It is useful to know which parasitics degrade the tuning performance so that devices which minimize the parasitics can be used. Likewise it is useful to know if any of the parameters enhance the tuning range so that they can be maximized in the varactor being used. The parasitics considered are those in Fig. 8:  $L_s$ ,  $L_p$ ,  $C_p$ , and  $R_s$ .  $R_s$  is the bulk resistance of the semiconductor and  $L_p$  and  $C_p$  are due to the varactor packaging. Typical values for  $R_s$ ,  $L_p$ , and  $C_p$  are given by manufacturers in their data books for a given device and package style.

The resonant frequency as a function of varactor capacitance has been plotted for various parameters in Figs. 11 through 13. The ranges for the parameters are typical values that can be expected for a packaged varactor.

In Fig. 11 the effect of the package capacitance on the resonant frequency is displayed. The packaged capacitance

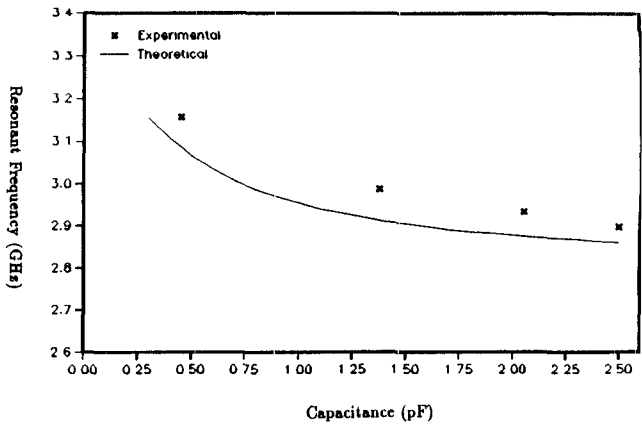


Fig. 9. Tuning range for a tunable and switchable ring resonator.

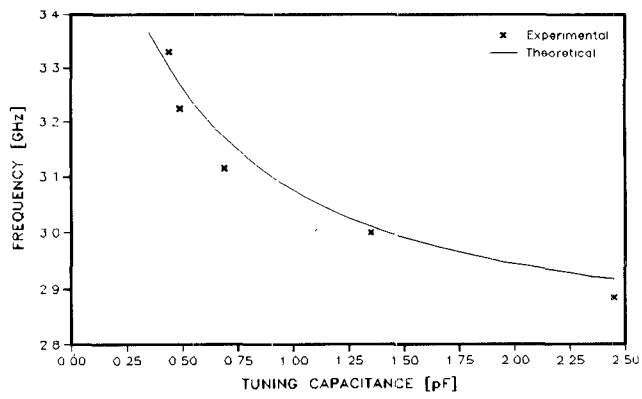
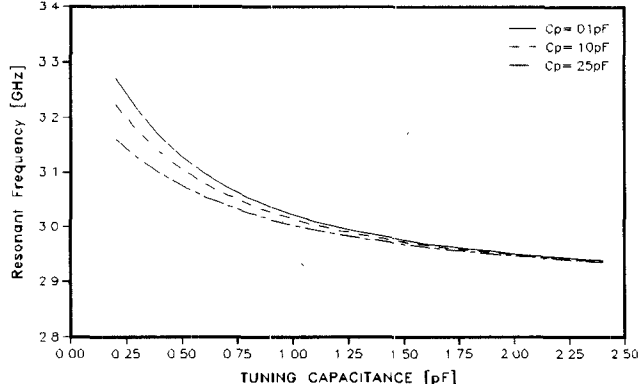


Fig. 10. Resonant frequency as a function of a varactor capacitance for a ring with two varactors.

Fig. 11. Effect of  $C_p$  on the resonant frequency as a function of tuning capacitance.

$C_p$  is in parallel with the tuning capacitance  $C_j$ . Because capacitances in parallel are added, the effective varactor capacitance (neglecting  $C_2$ ) can be written as  $C_p + C_j$ . From Fig. 11, it can be seen that for a small varactor junction capacitance the package capacitance can give a large change in the resonant frequency, while for a large junction capacitance the effect is small. If a package with a large package capacitance is used, then the device capacitance will be dominated by the package capacitance. The device junction capacitances will have less of an effect on the resonant frequency and the result is a smaller tuning

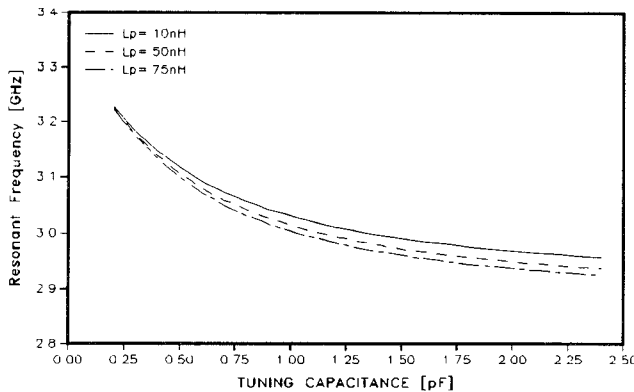


Fig. 12. Effect of  $L_p$  on the resonant frequency as a function of tuning capacitance.

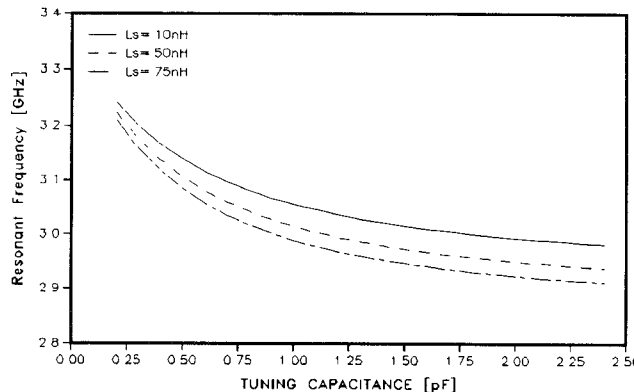


Fig. 13. Effect of  $L_s$  on the resonant frequency as a function of tuning capacitance.

range. As the package capacitance is increased while all other parameters remain constant, the frequency tuning range for a given capacitance range is smaller. To ensure the maximum tuning range possible it is important that a package with a small capacitance be chosen.

The inductance  $L_p$  is also introduced in the device package. Fig. 12 shows the effects of the package inductances on the resonant frequency. As the inductance is increased the tuning range is also slightly increased. The inductance does not degrade the performance of the circuit but seems to enhance it. It is generally conceived that all package parasitics should be minimized in order to maximize the performance of any circuit, but this is not the case for this application. Many package styles offer relatively high inductances (as high as 2.0 nH). In this varactor application the package inductance does not degrade the performance of the circuit; thus if given a choice, a package with a large inductance should be chosen.

The bonding inductance is not actually package parasitic in the strictest sense because it does not lie within the package itself. The inductance  $L_s$  arises from the embedding of the varactor into the circuit. The leads from the device to the circuit and the bonding of the leads give rise to  $L_s$ . Information on this inductance cannot be supplied by the vendor because it varies for each application. The effect of  $L_s$  on the resonant frequency is given in Fig. 13. The range of  $L_s$  is arbitrarily chosen but one would expect

$L_s$  to be at least comparable to  $L_p$  because of the physical dimensions involved. As can be seen in Fig. 13 the inductance  $L_s$  does not degrade the frequency tuning range and may actually improve it slightly. As the inductance is increased the whole tuning curve is lowered. This gives the same effect as increasing the mean circumference of the ring and, as would be expected, lowers the resonant frequency.

Theoretical results show that the bulk resistance  $R_s$  does not affect the resonant frequency of the circuit. It should be noted that it is important to minimize  $R_s$  so that the circuit  $Q$  will be as high as possible and the insertion loss kept as low as possible.

The effect of the package parasitics on the tuning range is summarized below. From this information a device and package can be chosen so that the frequency tuning range is maximized. The following guidelines can be used in choosing a varactor:

- 1) The tuning capacitance,  $C_j$ , should span a large range of junction capacitance values.
- 2) A package should be chosen such that the package capacitance,  $C_p$ , is as small as possible.
- 3) A package should be chosen such that the package inductance,  $L_p$ , is as large as possible.
- 4) The bonding wires will not degrade the tuning range but should be kept as short as possible so that  $L_s$  will be more predictable.
- 5) The bulk resistance should be as small as possible.

## V. CONCLUSIONS

Two novel microstrip ring resonator circuits have been developed. One uses two p-i-n diodes mounted inside the ring and works as a switchable filter. The other works as a tunable switchable filter using one p-i-n diode together with a varactor. An isolation of over 20 dB and a tuning bandwidth of 9 percent were achieved. The resonant frequency and tuning bandwidth agree very well with a theoretical analysis based on transmission line modeling. The analysis includes the effects of diode parasitics, coupling gaps, dispersion, and mounting gap capacitance. The effects of varactor package parasitics on the tuning range have also been investigated using this analysis. Although no attempt was made to match the circuits using the analysis, matching networks can be easily designed since the input impedance can be calculated. The results should have many system applications in hybrid and monolithic circuits.

## ACKNOWLEDGMENT

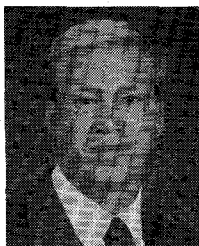
The authors would like to thank Dr. H. Taylor for many helpful suggestions and encouragement.

## REFERENCES

- [1] P. Troughton, "High  $Q$ -factor resonator in microstrip," *Electron Lett.*, vol. 4, pp. 520-522, 1968.
- [2] P. Troughton, "Measurement techniques in microstrip," *Electron Lett.*, vol. 5, pp. 25-26, 1969.
- [3] T. C. Edwards, "Microstrip measurements," in *IEEE MTT-S Int. Microwave Symp. Dig.*, 1982, pp. 338-341.

- [4] H. J. Finlay *et al.*, "Accurate characterization and modelling of transmission lines for GaAs MMIC's," in *IEEE MTT-S Int. Microwave Symp. Dig.*, 1986, pp. 267-270.
- [5] M. Makimoto and M. Sagawa, "Varactor tuned bandpass filters using microstrip-line resonators," in *1986 IEEE MTT-S Int. Microwave Symp. Dig.*, June 1986, pp. 411-414.
- [6] K. Chang, T. S. Martin, F. Wang, and J. L. Klein, "On the study of microstrip ring and varactor-tuned ring circuits," *IEEE Trans. Microwave Theory Tech.*, vol. MTT-35, pp. 1288-1295, Dec. 1987.
- [7] I. Wolff and N. Knoppik, "Microstrip ring resonator and dispersion measurements on microstrip lines," *Electron. Lett.*, vol. 7, pp. 779-781, Dec. 1971.
- [8] R. P. Owens, "Curvature effect in microstrip ring resonators," *Electron. Lett.*, vol. 12, pp. 336-357, July 1976.
- [9] S. G. Pintzos and R. Pregla, "A simple method for computing the resonant frequencies of microstrip ring resonators," *IEEE Trans. Microwave Theory Tech.*, vol. MTT-26, pp. 809-813, Oct. 1978.
- [10] Y. S. Wu and F. J. Rosenbaum, "Mode chart for microstrip ring resonators," *IEEE Trans. Microwave Theory Tech.*, vol. MTT-21, pp. 487-489, July 1973.
- [11] V. K. Tripathi and I. Wolff, "Perturbation analysis and design equations for open- and closed-ring microstrip resonators," *IEEE Trans. Microwave Theory Tech.*, vol. MTT-32, pp. 405-409, Apr. 1984.
- [12] I. Wolff and V. K. Tripathi, "The microstrip open-ring resonator," *IEEE Trans. Microwave Theory Tech.*, vol. MTT-32, pp. 102-106, Jan. 1984.

✖



**T. Scott Martin** was born in Levelland, TX, on March 6, 1964. He received the B.S. and M.S. degrees in electrical engineering from Texas A&M University in 1986 and 1987, respectively.

He joined the Microwave Laboratory of Texas Instruments in 1988, where he is currently working on monolithic microwave circuit modeling and development.

In 1987 Mr. Martin received the IEEE-MTT Fellowship. He is a member of Eta Kappa Nu.

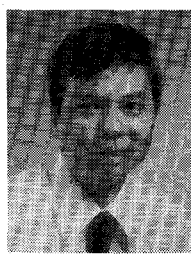
✖

**Fuchen Wang** was born in Jilin, China, on February 18, 1936. He graduated from Qinghua University, Beijing, China, in 1963.

From 1963 to 1968 he was with the Hebei Semiconductor Research Institute, China, where he was engaged in the design, fabrication, and testing of microwave mixer diodes. In 1968 he joined the Nanjing

Solid-State Devices Research Institute. From 1968 to 1979 he was a Group Head working in the area of microwave and millimeter-wave Gunn and IMPATT oscillators. From 1979 to 1985 he was vice director of a laboratory working on the development of GaAs microwave monolithic integrated circuits. Since 1985 he has been an Engineering Research Associate in the Department of Electrical Engineering at Texas A&M University doing research on microwave integrated circuits.

✖



**Kai Chang** (S'75-M'76-SM'85) received the B.S.E.E. degree from National Taiwan University, Taipei, Taiwan, in 1970, the M.S. degree from the State University of New York at Stony Brook in 1972, and the Ph.D. degree from the University of Michigan, Ann Arbor, in 1976.

From 1972 to 1976 he worked for the Microwave Solid-State Circuits Group, Cooley Electronics Laboratory of the University of Michigan as a research assistant. From 1976 to 1978 he was employed by Shared Applications, Ann Arbor, where he worked on computer simulation of microwave circuits and microwave tubes. From 1978 to 1981, he worked for the Electron Dynamics Division, Hughes Aircraft Company, Torrance, CA, where he was involved in the research and development of millimeter-wave devices and circuits. This activity resulted in state-of-the-art IMPATT oscillator and power combiner performance at 94, 140, and 217 GHz. Other activities included silicon and gallium arsenide IMPATT diode design and computer simulation, Gunn oscillator development, and monopulse comparator and phase shifter development. From 1981 to 1985 he worked for the TRW Electronics and Defense, Redondo Beach, CA, as a section head in the Millimeter-Wave Technology Department, developing state-of-the-art millimeter-wave integrated circuits and subsystems including mixers, VCO's, transmitters and amplifiers, modulators, upconverters, switches, multipliers, receivers, and transceivers. He joined the Electrical Engineering Department of Texas A&M University in August 1985 as an Associate Professor and was promoted to Professor in 1988. His current interests are in microwave and millimeter-wave devices and circuits, microwave optical interactions, and radar systems.

Dr. Chang is the editor of the *Handbook of Microwave and Optical Components*, to be published by Wiley & Sons, Inc. He is also editor of *Microwave and Optical Technology Letters*. He has published more than 80 technical papers, as well as three book chapters and 14 government reports, in the areas of microwave and millimeter-wave devices and circuits.